A hypothetical polymorph of copper(II) guanidinium formate

Shurong Yuan,[1] Alessandro Stroppa,[2] and Anthony E. Phillips[1]
[1)] *School of Physical and Chemical Sciences, Queen Mary University of London, London E1 4NS, U.K.*
[2)] *Consiglio Nazionale delle Ricerche, Institute for Superconducting and Innovative Materials and Devices (CNR-SPIN), c/o Department of Physical and Chemical Sciences, University of L'Aquila, Via Vetoio I-67100 Coppito, L'Aquila, Italy*

The hybrid perovskite copper(II) guanidinium formate, $C(NH_2)_3[Cu(HCO_2)_3]$, is a close analogue of the inorganic material $KCuF_3$, a well-studied exemplar of the Heisenberg spin-$\frac{1}{2}$ antiferromagnetic chain. However, the polymorphism known in $KCuF_3$, based on different orbital ordering of the d^9 Cu^{2+} ions, has never been observed in $C(NH_2)_3[Cu(HCO_2)_3]$. We use density-functional theory calculation to construct a hypothetical polymorph of the hybrid perovskite analogous to the known structure of $KCuF_3$. This polymorph is very similar in geometric and magnetic structure to the known phase of $C(NH_2)_3[Cu(HCO_2)_3]$, but is no longer polar. It has only a marginally higher internal energy than the known phase, but also a lower vibrational entropy and hence a higher free energy. Furthermore, stacking faults are far more energetically costly in $C(NH_2)_3[Cu(HCO_2)_3]$ than $KCuF_3$. These results together help to explain why $KCuF_3$ is experimentally polymorphic but $C(NH_2)_3[Cu(HCO_2)_3]$ is not. The detailed comparison between analogous inorganic and hybrid materials illustrates the subtle differences that can arise from replacing atomic by molecular ions, and that may be exploited in crystal engineering of these materials.

I. INTRODUCTION

One of the most promising recent approaches to materials discovery is to expand a simple inorganic structure by replacing individual atoms by entire molecules. For instance, solid argon has the cubic close-packed structure.[1] The tetrahedral molecule adamantane ($C_{10}H_{16}$)[2] and the truncated icosahedron of C_{60} buckyballs[3] are, to a good approximation, spherically symmetric; and, like argon atoms, these molecules interact with their neighbours primarily through van der Waals forces. It is not surprising, therefore, that by replacing argon atoms by adamantane or buckminsterfullerene molecules, we can construct plausible cubic close-packed structures of these materials, which indeed are experimentally verified at temperatures high enough that the molecular deviations from spherical symmetry are insignificant.

Among the most significant examples of this approach is the family of "hybrid" or "molecular perovskites". Like the inorganic minerals that bear the same name, these materials have the topology of a cubic network, with "*B*-site" cations octahedrally coordinated to "*X*-site" linker anions while "*A*-site" cations sit in the cubic interstices. The inorganic materials are well known for their propensity to undergo structural distortions: for instance, the BX_6 octahedra may cooperatively tilt, or alternatively distort by off-centring of the central *B* cation, or by tetragonal deformations typically due to the Jahn-Teller (JT) effect in the partially occupied 3*d* subshell. This leads to a wide variety of known phases, many of which have important functionality.[4] It turns out that the principle of replacing atomic by molecular ions can be carried out at each of the *A*, *B*, and *X* sites; indeed, solid solutions are possible at each of these sites. Incorporating polyatomic ions into an already rich class of compounds thus produces an extraordinarily large and diverse new family of functional materials.[5,6]

An important consequence of replacing atoms by molecules to form the molecular perovskites is simply that the size of the unit cell is thereby increased. Indeed, many principles well established in the world of the inorganic perovskites, such as Goldschmidt's tolerance factor, apply with only slight adjustments to the molecular analogues as well.[7,8] However, there are many other important differences between the molecular and inorganic perovskites. Simply moving from a monatomic to a polyatomic *X*-site linker effectively decouples the rotation of adjacent BX_6 octahedra. This allows new distortion modes that were not previously possible, including "forbidden" octahedral tilting, where adjacent octahedra rotate in the same sense while the linker that joins them rotate in the opposite direction; and columnar shifts, where columns of octahedra translate along their length rather than rotating.[9,10] In general, the decreased site symmetry leads to an increase in the number of thermodynamically accessible degrees of freedom.[11]

This new freedom is not simply a crystallographic curiosity. The combination of these distortion modes can produce interesting and important functionality, such as "hybrid improper ferroelectricity", where two or more individually non-polar modes combine to give a net electric polarisation.[12] This naturally motivates crystal structure prediction efforts to discover new functional phases that can be synthesised. From a practical materials discovery perspective, though, it can be equally important to discover why apparently plausible phases are *not* experimentally realisable. Here we present an study of this second sort, investigating why an inorganic perovskite with two polymorphs has a molecular analogue for which only one polymorph is known.

II. TARGET MATERIAL

Potassium copper(II) fluoride, $KCuF_3$, is an orbital-ordered inorganic perovskite that has become the paradigmatic example of a one-dimensional Heisenberg spin-$\frac{1}{2}$ antiferromagnetic chain.[13–19] According to the perovskite topology, each copper ion has an octahedral coordination environment and is thus connected to its neighbours in all three dimensions. However, the cooperative JT effect gives rise to a ground state that allows appreciable superexchange only along one direction (the crys-

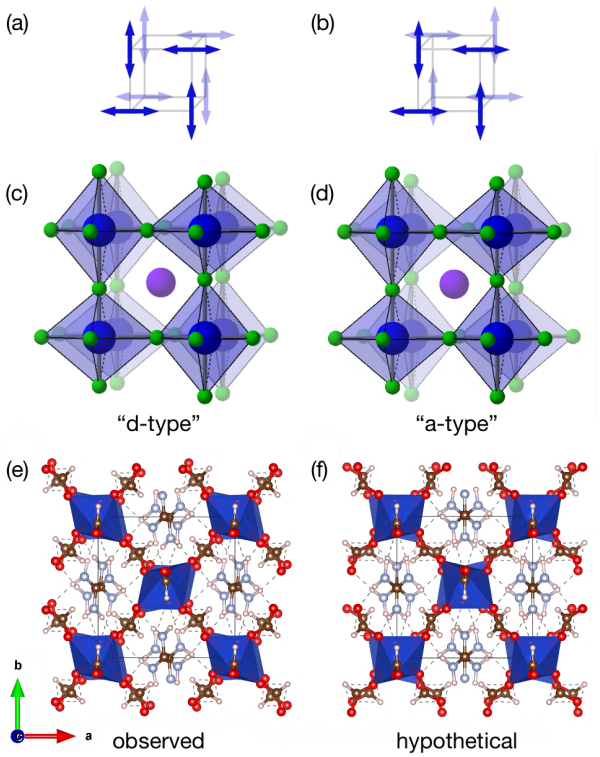

FIG. 1. (a,b) Schematic diagrams of the two possible cooperative JT distortion modes, consistent with the geometric criterion that no two adjacent Cu atoms should both have "long" bonds along the vector between them. Corresponding structures of (c) *d*- and (d) *a*-type $KCuF_3$ (Cu: deep blue; K: purple; F: green), and of (e) the observed $Pna2_1$ phase and (f) the hypothetical $P2/a$ phase of $GuaCuFm_3$ (Cu: deep blue; O: red; C: brown; N: light blue; H: pink).

tallographic *c* axis), so that the material can be well modelled in terms of one-dimensional spin chains. Each $3d^9$ Cu^{2+} ion has two "long" (*l*), two "medium" (*m*) and two "short" (*s*) bonds connecting to the *X*-site F^- ions. Along two of the pseudocubic perovskite cell axes, corresponding to the interchain interactions, *l* and *s* bonds alternate, with little magnetic exchange; the third axis, corresponding to intrachain interactions, contains chains of *m* bonds with strong magnetic exchange.

A well-studied molecular analogue to $KCuF_3$ is guanidinium copper(II) formate, $C(NH_2)_3[Cu(HCO_2)_3]$ ($GuaCuFm_3$).[20] This has an almost exactly equivalent structure, with guanidinium ($C(NH_2)_3^+$) replacing the potassium and formate (HCO_2^-) replacing the fluoride, and indeed it similarly exhibits one-dimensional spin chains. However, in contrast to the centrosymmetric $KCuF_3$, exactly the hybrid improper mechanism discussed above gives rise to a polar structure in $GuaCuFm_3$.[12] This allows an interesting and important range of new properties in $GuaCuFm_3$, including magnetoelectric coupling, which was predicted on the basis of *ab initio* calculations[21,22] before being confirmed experimentally.[23]

In fact, $KCuF_3$ has two polymorphs, which differ in the stacking arrangement along the *c* axis, the direction of the spin chains. The two polymorphs have different ordering of the *l* bonds looking down these spin chains, either having the *l* bonds alternate between the two possible directions (*a*-type $I4/mcm$) or having them lie on top of one another (*d*-type $P4/mbm$) (figure 1). They have similar one-dimensional magnetic properties with slightly different Néel temperatures.[24] The two polymorphs are similar enough in structure and energy to make intermediate structures between the two possible.[25] In the language of group representation theory, using a setting of the ideal $Pm\bar{3}m$ perovskite structure with the **B**-site cation at the origin, these distortions transform respectively according to the R_3^+ (*a*-type) and M_2^+ (*d*-type) irreps.

Given the close analogy between $KCuF_3$ and $GuaCuFm_3$, one might expect that the coordination framework too has multiple polymorphs. However, only one polymorph of $GuaCuFm_3$ has been experimentally reported. This corresponds to the *less* stable $P4/mbm$ polymorph of $KCuF_3$, or the M_2^+ irrep. In fact, the space group actually observed for $GuaCuFm_3$ is $Pna2_1$, which incorporates conventional tilting of the octahedra, columnar shifts, and multipolar order on the A site, as well as the cooperative JT distortion.

Here, by analogy with $KCuF_3$, we construct the "missing" polymorph of $GuaCuFm_3$. There are at least four possible reasons why this structure has never been experimentally observed: it might be unfavourable because of a high internal energy due to its (1) atomic or (2) magnetic structure, or (3) intermediate structures (stacking faults) between the two polymorphs; or because (4) of a high free energy arising from entropic contributions. We investigate these possibilities by density functional theory (DFT) simulation. We show that the difference between the ground-state energies is small, so that entropic and kinetic effects are likely to be dominant in preventing this structure from being experimentally realised.

III. METHODS

DFT calculations were performed using the CASTEP software package.[26] A plane-wave basis set together with norm-conserving pseudopotentials from the CASTEP standard library were used.[27] The energy cutoff was set to 800 eV, and the Brillouin zone was sampled in a $2\times2\times2$ Monkhorst-Pack *k*-point grid.[28] The PBEsol functional[29] was used to describe the exchange-correlation energy, along with the Tkatchenko-Scheffler[30] semi-empirical dispersion correction[31] to account for non-bonded interactions. A Hubbard *U* parameter of 4 eV was applied to the Cu $3d$ electrons. Geometry optimisations[32] using the LBFGS algorithm[33] were continued until the change in energy per ion was less than 2×10^{-5} eV, the maximum force was less than 5×10^{-3} eV Å^{-1}, the maximum displacement of any atom between cycles was less than 1×10^{-3} Å, and the maximum stress was less than 0.1 GPa. A finite basis set correction was applied to account for Pulay forces.[34]

IV. CONSTRUCTION OF A NEW POLYMORPH

First, the experimental structure and cell were optimised using the experimentally determined $Pna2_1$ symmetry.[20] Next,

	$Pna2_1$ (expt.)[20]	$Pna2_1$ (calc.)	$P2/a$
a (Å)	8.5212(3)	8.767	8.682
b (Å)	9.0321(3)	9.038	9.044
c (Å)	11.3497(4)	11.310	11.309
β (°)	90	90	92.3
V (Å^3)	873.52(9)	896.2	887.3

TABLE I. Optimised cell parameters in the two calculated phases, and as experimentally reported.

the symmetry of the relaxed structure was reduced to $P1$ – *i.e.*, keeping only the translational symmetry associated with crystalline periodicity – and the formate anions were manually shifted to artificially distort the Cu – O distances, in such a way that *l* and *s* bonds alternate looking down the *c* axis. The Gua^+ cations were also adjusted slightly to maintain as far as possible the $Gua^+\cdots Fm^-$ hydrogen bonding in the original $Pna2_1$ phase. The resulting structure and cell were then relaxed, still in $P1$. Next, the *PSEUDO* tool of Bilbao Crystallographic Server was used to determine the true space group of the newly constructed polymorph.[35] We found that this structure was very well described, within numerical error, by the space group $P2/a$: the maximum distance between sites in $P1$ that are equivalent in $P2/a$ was $\Delta_{\max} = 0.4$ Å, so that the greatest distance moved by any atom when "snapping" to a high-symmetry site was 0.2 Å. Finally, the structure and cell were once again optimised in $P2/a$. (We use a non-standard setting of space group no. 13, $P2/c$, in order to maintain axis labels consistent with the $Pna2_1$ phase.)

The final structure obtained in this way indeed satisfies the construction criteria, that the JT distortion corresponds to the R_3^+ irrep, analogous to *a*-type $KCuF_3$, and the hydrogen bonding network remains intact. The structures of the $Pna2_1$ and $P2/a$ phases are shown in figure 1 (e) and (f); the lattice parameters are presented in Table I. The hydrogen bond network is an important feature of all the $GuaMFm_3$ systems, with the snug fit between *A*-site Gua^+ cations and *X*-site Fm^- anions contributing to the structural rigidity.[36] In our DFT calculation, the $Pna2_1$ phase shows hydrogen bond lengths ranging from 1.800 to 2.035 Å, with an average of 1.907 Å; the hydrogen bonds in the $P2/a$ phase turn out to have a more concentrated length range, ranging from 1.811 to 1.948 Å, with a slightly lower average of 1.898 Å.

The magnetic properties of the newly constructed $P2/a$ phase were determined by calculating the DFT energies of four possible spin configurations, corresponding to ferromagnetism and *A*-, *C*-, and *G*-type antiferromagnetism. The lowest-energy configuration was found to be *A*-type antiferromagnetism, with adjacent Cu^{2+} ions along the spin-chains parallel to *c* interacting antiferromagnetically, while Cu^{2+} ions lying in the same *ab* plane have the same spin direction. This is the same structure as reported for the $Pna2_1$ phase.[21]

Using the Heisenberg Hamiltonian

$$H = \frac{1}{2}\sum_{ij} J_{ij}\mathbf{S}_i \cdot \mathbf{S}_j + E_0, \qquad (1)$$

where the sum runs over all neighbouring atoms, the exchange coupling within the *ab* plane is

$$J_{ab} = -\frac{1}{32\mathbf{S}^2}\left(H_{\text{FM}} + H_{A\text{-AFM}} - H_{C\text{-AFM}} - H_{G\text{-AFM}}\right) \qquad (2)$$

and along the *c* axis is

$$J_c = -\frac{1}{16\mathbf{S}^2}\left(H_{\text{FM}} + H_{C\text{-AFM}} - H_{A\text{-AFM}} - H_{G\text{-AFM}}\right), \qquad (3)$$

where in each case H refers to the energy of a unit cell consisting of 4 formula units of $GuaCuFm_3$. This gives a ratio $J_{ab}/J_c = -0.06$ for $Pna2_1$ and $J_{ab}/J_c = -0.07$ for $P2/a$, again showing very similar magnetic behaviour.

V. SYMMETRY-MODE ANALYSIS

In order to compare these two polymorphs in a more systematic way, we performed symmetry-mode analysis using the *ISODISTORT*[37] software, which projects a distorted structure onto the symmetry modes of a given parent. An amplitude, defined simply as the root-mean-square displacement of the atoms in the distorted structure with respect to the parent structure, can thus be calculated for each mode. This analysis naturally reveals different aspects of the target structure, depending on the parent structure chosen. We present here two versions: the first with respect to the aristotype perovskite structure; the second in terms of the minimal supergroup containing the symmetry of both polymorphs, to accentuate the differences between them.

First, we report the analysis in terms of the aristotype perovskite structure, which has space group $Pm\bar{3}m$. In both polymorphs, compared to an atomic A-site cation, the guanidinium ion breaks symmetry in two ways: a quadrupolar ordering associated with the orientation of the normal to the ionic plane, and a hexadecapolar ordering associated with rotation about this normal.[12] To avoid dealing with molecular disorder in the parent phase – for which a mode amplitude would be more or less meaningless – and since our interest here is primarily in the distortion of the metal-formate framework, we removed the guanidinium ion from our analysis. The parent framework was constructed with an unphysical, linear "formate" ion for consistency with the cubic symmetry: its asymmetric unit consisted of a Cu atom at $(0,0,0)$, O at $(0.3,0,0)$ and both H and C atoms at $(0.5,0,0)$.

The results of this analysis are shown in Table II. In addition to the expected Jahn-Teller modes M_2^+ and R_3^+, the principal distortions come from conventional tilting of the octahedra (R_4^+) and columnar shifts (X_5^-). ("Conventional" here indicates that this mode would be possible even with a monatomic linker.) In each case, the amplitudes of corresponding modes are rather similar between the two polymorphs; the Jahn-Teller distortion is slightly smaller in the hypothetical $P2/a$ structure than the known $Pna2_1$ structure.

As a second version of this analysis, in order to isolate the specific modes associated with Jahn-Teller distortion, we now consider instead a parent structure of lower symmetry. In contrast to the first symmetry-mode analysis presented above,

Amplitude (Å)		$Pm\bar{3}m$			$Imam$		
		M_2^+ / R_3^+	R_4^+	X_5^-	X_4^+ / Γ_2^+	X_1^-	Γ_4^- / X_2^-
$KCuF_3$	$P4/mbm$ (d-type)	0.376 (M)	\		\		
	$I4/mcm$ (a-type)	0.373 (R)					
$GuaCuFm_3$	$Pna2_1$	1.303 (M)	4.940	3.518	1.706 (X)	6.617	0.548 (Γ)
	$P2/a$	1.158 (R)	4.933	3.468	1.262 (Γ)	6.585	0.522 (X)

TABLE II. Mode amplitudes of two polymorphs for both $KCuF_3$ and $GuaCuFm_3$. With the reference space group as $Pm\bar{3}m$, M_2^+ and R_3^+ correspond to JT distortion; R_4^+: conventional tilting of the octahedra; X_5^-: columnar shift; secondary modes are not shown in the table. With the reference space group as $Imam$, X_4^+ and Γ_2^+: JT distortion; X_1^-: rotation of Gua^+; Γ_4^- and X_2^-: secondary mode.

this allows us to include all atoms, including the guanidinium ions. The minimal supergroup of the two polymorphs, $Pna2_1$ and $P2/a$, is $Pnna$. This is also the experimentally observed space group of the analogous guanidinium formate framework with Jahn-Teller inactive metal ions (Mn, Fe, Co, Ni, Zn).[20] However, we take the higher-symmetry group $Imma$ as the parent phase in order to investigate the coupling between Jahn-Teller distortion and guanidinium ion orientation. For the same reason, the $Imma$ structure was used as the reference phase in a previous analysis of ferroelectricity in the hypothetical material $GuaCrFm_3$.[22] Once again adopting a non-standard setting to preserve the axis orientations, we consider the parent structure in $Imam$.

The Bärnighausen trees showing the descent of symmetry from the $Imam$ parent phase to the two polymorphs are shown in Figure 2, and the corresponding mode amplitudes are tabulated in Table II. For each polymorph, the two main distortion modes are the Jahn-Teller distortion (X_4^+ and Γ_2^+, respectively) and ordering of the guanidinium ions, specifically their rotation away from the ab plane (X_1^-); there is also a secondary mode, with smaller amplitude, that arises from coupling between these two modes (Γ_4^- and X_2^-, respectively). The mode amplitudes for the $Pna2_1$ phase are consistent with those previously reported for $GuaCrFm_3$.[38] Once again, the mode amplitudes for the hypothetical $P2/a$ phase are similar to those for $Pna2_1$, with less Jahn-Teller distortion in $P2/a$. Note that, of course, the irrep labels here are different from those in the previous analysis, because they are taken with respect to different parent phases. In particular, the propagation vector X here corresponds to a cell doubling along the c-axis: that is, along the spin-chain direction.

A point of interest in this symmetry analysis is that $Pna2_1$ $GuaCuFm_3$ is a hybrid improper ferroelectric, in which the polar structure arises from coupling between two non-polar distortion modes (X_4^+ and X_1^-).[38] Since any term in a Landau free energy expansion must have the full symmetry of the parent phase, it follows that any such coupling (between exactly two non-polar modes) must involve a polar distortion with symmetry Γ^- and two modes with the *same* propagation vector but opposite behaviour on inversion: for instance, an X^+ and an X^- mode. These are, of course, the X_4^+, X_1^- and Γ_4^- modes depicted in Figure 2(a).[12]

It is therefore the fact that the guanidinium ordering causes precisely the same cell doubling as does the JT distortion that is responsible for the ferroelectric ordering. By contrast, the Γ_2^+ and X_1^- modes are prevented by symmetry from coupling with a polar distortion, and indeed we find that the hypothetical phase in which these modes are active has the non-polar space group $P2/a$. A different arrangement of the guanidinium ions would alter which JT distortion modes yield polar phases.

At least one example of this is known experimentally: the Cd analogue $GuaCdFm_3$ has a structure with space group $R\bar{3}c$ in which all of the guanidinium ions are parallel.[39] A 50% solid solution between Cd and Cu maintains this "R-type" guanidinium ordering while introducing d-type JT distortion, giving a structure with the *non-polar* space group $P2_1/c$.[40] This is not a perfect analogy with the orthorhombic phase discussed here, because no rotation of the guanidinium ions is needed between the high-symmetry centrosymmetric phase and the JT distorted phase; thus even combining R-type guanidinium ordering with a-type JT distortion to form another hypothetical polymorph (which we consider further below) would give the non-polar space group $C2/c$. Nonetheless, this illustrates the point that it is the combination of the A-site ordering with the JT distortion that gives rise to the observed polar structure. It is intriguing to speculate that different A-site ordering, perhaps arising from different choices of A-site or linker ions, could stabilise a different orbital ordering.

VI. RELATIVE STABILITY OF THE POLYMORPHS

We now return to the question of why the hypothetical $P2/a$ polymorph of $GuaCuFm_3$ is not observed experimentally.

First, we consider the internal energy of the two polymorphs. The $P2/a$ structure has energy 9.5 meV/fu greater than $Pna2_1$, which is a potentially significant but not overwhelming difference. For comparison, we find using calculations at the same level of theory that in $KCuF_3$, the a-type $I4/mcm$ phase is more stable than the d-type $P4/mbm$ phase by 2.5 meV/fu.

Second, we include a simple vibrational analysis to calculate instead the free energy. Given the large system of 92 atoms per unit cell, we used the finite displacement method to calculate the phonon modes at the Γ point only. Neither phase shows any imaginary frequencies, confirming their stability. The phonon free energy is calculated using the relationship

$$F_{\mathrm{vib}} = \frac{1}{2}\sum_i \hbar\omega_i + k_{\mathrm{B}}T\sum_i \ln\left(1-\exp(-\hbar\omega_i/k_{\mathrm{B}}T)\right) \qquad (4)$$

where the summation runs through harmonic vibrational modes with angular frequencies ω_i.[41] The $Pna2_1$ phase is likewise lower in free energy at all temperatures, with a minimum difference of 37 meV/fu at $T = 50$ K (Fig. 3). The phonon modes

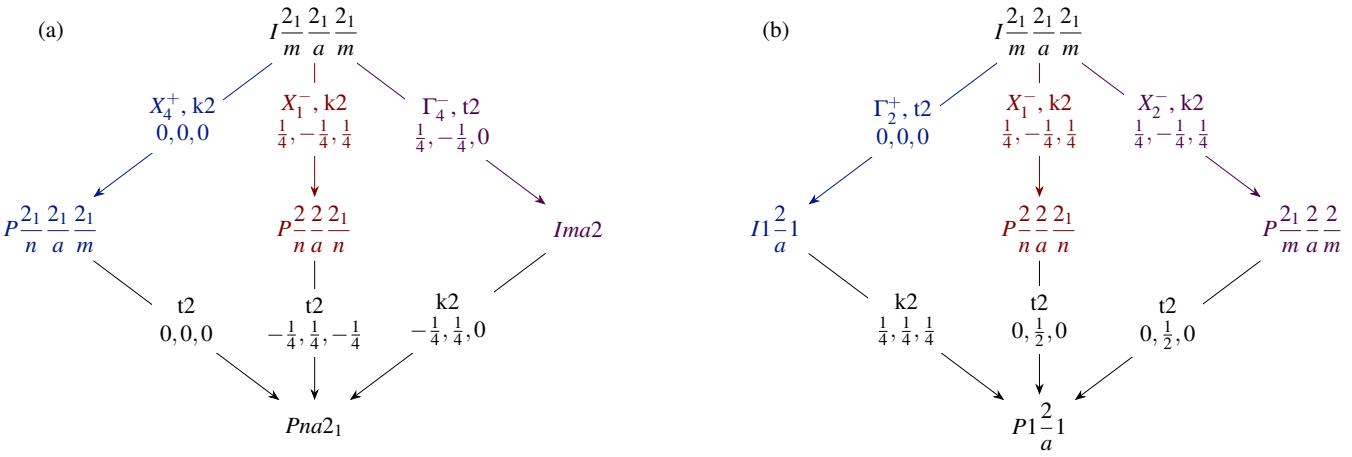

FIG. 2. Bärnighausen trees showing the modes that distort the parent *Imam* to form (a) $Pna2_1$ and (b) $P2/a$ phases. JT distortion modes are shown in blue, guanidinium rotation modes in red, secondary modes arising from coupling between these in purple. The symmetry labels of the active irreps are given with respect to the parent *Imam* phase. Unconventional settings are chosen where necessary so that the unit cell vectors do not change throughout these transformations; the coordinates given represent changes in origin. Each transition is labelled twofold *klassengleiche* (k2) or twofold *translationengleiche* (t2).

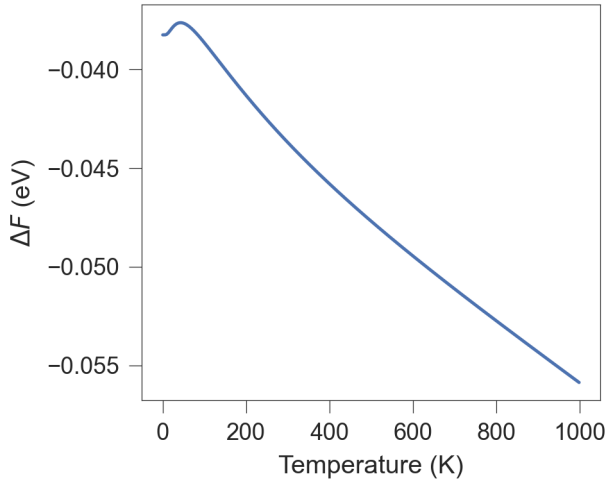

FIG. 3. Free energy difference between the polymorphs, $F_{Pna2_1} - F_{P2/a}$, as a function of temperature.

of both phases are extremely similar; the very small increase in phonon frequencies, and hence decrease in entropy, of the $P2/a$ structure compared to $Pna2_1$ may simply be a result of the small decrease in volume (Table I). Although it is important to acknowledge the limitations of considering only Γ-point frequencies rather than the overall Brillouin zone, this analysis is again consistent with the experimental observation of only the $Pna2_1$ polymorph.

Third, in $KCuF_3$, stacking faults can produce intermediate structures between the two polymorphs.[25] We therefore explore the same possibility in $GuaCuFm_3$. Recall that for the $Pna2_1$ phase, looking down the *c* axis, each unit cell has two layers of distorted octahedra, with each layer having the same distortion direction (Fig. 1c); this can be labelled an *aa* stacking pattern. On the other hand, in $P2/a$ the two layers of octahedra are distorted in different directions (Fig. 1d), giving *ab* stacking. Based on these layer differences, an intuitive way of constructing a stacking fault is to build a $1\times1\times2$ supercell with *aabb* layers of octahedra. This supercell alternately consists of two continuous layers with the same distortion direction (*aa* or *bb*) as in $Pna2_1$, and two with different directions (*ab* or *ba*) as in $P2/a$. It can therefore be regarded as a simple "1+1" stacking of the $Pna2_1$ and $P2/a$ polymorphs, and the energetic cost of a stacking fault can be determined from

$$\Delta E = E_{\text{supercell}} - (E_{aa} + E_{ab}) \tag{5}$$

Evaluating this shows that a stacking fault in $GuaCuFm_3$ costs $18.0\,\text{meV/fu}$ with respect to the two components. For comparison, we again perform the same analysis on $KCuF_3$, giving a difference of $-0.1\,\text{meV/fu}$, suggesting a very slight energetic *preference* for such faults. Again, this simple analysis is qualitatively consistent with the experimental observation that stacking faults are often found in $KCuF_3$ but have not been reported in $GuaCuFm_3$. This difference may also be a result of the different synthetic methods used: $GuaCuFm_3$ crystals are typically grown from aqueous solution, which will enable faults to dissolve and self-correct more readily than $KCuF_3$ growth from the melt.

As noted in the previous section, one might imagine another hypothetical polymorph, with space group $C2/c$, that combines R-type guanidinium ordering with *a*-type JT distortion. Geometry optimisation of this structure in the same way shows that it has an internal energy $21.4\,\text{meV/fu}$ greater than the $Pna2_1$ structure, and furthermore that it has several unstable zone-centre distortion modes. For this reason, we expect that this polymorph is unlikely to be experimentally realisable and have not investigated it further.

VII. CONCLUSION

Inspired by polymorphism in the inorganic perovskite $KCuF_3$, we have constructed a new polymorph of the well-studied molecular analogue $GuaCuFm_3$ with an orbital ordering pattern different from that observed experimentally. The hypothetical $P2/a$ phase and experimentally reported $Pna2_1$ phase are predicted to have the same perovskite topology, similar framework geometries and hydrogen-bonding connections, and the same *A*-type antiferromagnetic configuration. However, as predicted on group-theoretical grounds, the hypothetical phase does not display the same hybrid improper ferroelectric behaviour as the experimentally known material. The experimental $Pna2_1$ phase is only slightly lower in internal energy, but is stabilised further by vibrational entropy. Furthermore, stacking faults that might introduce some character of the new distortion pattern into a crystal are substantially more energetically costly in $GuaCuFm_3$ than in $KCuF_3$.

The broad family of molecular perovskites is well known for the novel degrees of freedom that are introduced by replacing atomic by molecular ions, including new types of polymorphism.[42] However, the case of $GuaCuFm_3$ demonstrates that this substitution can also lead to a *loss* of some degrees of freedom: the rich landscape of partially ordered materials between the two polymorphs of the inorganic perovskite $KCuF_3$ appears not to be accessible to its molecular analogue. Our calculations indicate that this is not due to a large internal energy difference between the observed and hypothetical phases of $GuaCuFm_3$, but caused indirectly by differences in vibrational entropy and hence free energy, and in the energetic cost of stacking faults. Indeed, vibrational entropy is increasingly recognised as an important and even predominant contributor to stabilising particular phases in the molecular perovskites more generally.[43]

Our work suggests that judicious choices of the A-site (guanidinium) and/or linker (formate) ions may help to stabilise particular structures and types of orbital order more strongly than is possible in the inorganic perovskites. Such states may be of interest in their own right, as exemplars of magnetic models such as in $KCuF_3$, and may further lead to emergent effects such as hybrid improper ferroelectricity. These desiderata will add to the many targets already identified for crystal engineering of this large and diverse family of materials.

ACKNOWLEDGMENTS

We thank Kunihiro Yananose for useful discussions about the magnetic coupling calculations. SY thanks the China Scholarship Council for a studentship. The authors are grateful to the Royal Society for funding under the International Exchange programme (IES\R1\180034). For computational resources, we thank the UK Materials and Molecular Modelling Hub, which is partially funded by EPSRC (EP/T022213/1, EP/W032260/1 and EP/P020194/1).

SUPPLEMENTARY MATERIAL

The optimised structure and calculated phonon modes at Γ for both the $Pna2_1$ and $P2/a$ polymorphs are provided in plain-text format, as CASTEP `.phonon` files.

AUTHOR DECLARATIONS

The authors have no conflicts of interest to disclose.

[1] F. Simon and C. von Simson, "Die Kristallstruktur des Argons," Z. Phys. **25**, 160–164 (1924).
[2] C. E. Nordman and D. L. Schmitkons, "Phase transition and crystal structures of adamantane," Acta Crystallogr. **18**, 764–767 (1965).
[3] P. A. Heiney, J. E. Fischer, A. R. McGhie, W. J. Romanow, A. M. Denenstein, J. P. McCauley Jr., A. B. Smith, and D. E. Cox, "Orientational ordering transition in solid C_{60}," Phys. Rev. Lett. **66**, 2911–2914 (1991).
[4] R. J. D. Tilley, *Perovskites: Structure-Property Relationships* (John Wiley and Sons, Chichester, 2016).
[5] W. Li, Z. Wang, F. Deschler, S. Gao, R. H. Friend, and A. K. Cheetham, "Chemically diverse and multifunctional hybrid organic–inorganic perovskites," Nat. Rev. Mater. **2**, natrevmats201699 (2017).
[6] G. Kieslich and A. L. Goodwin, "The same and not the same: Molecular perovskites and their solid-state analogues," Mater. Horiz. **4**, 362–366 (2017).
[7] G. Kieslich, S. Sun, and A. K. Cheetham, "Solid-state principles applied to organic–inorganic perovskites: New tricks for an old dog," Chem. Sci. **5**, 4712–4715 (2014).
[8] G. Kieslich, S. Sun, and A. K. Cheetham, "An extended Tolerance Factor approach for organic–inorganic perovskites," Chem. Sci. **6**, 3430–3433 (2015).
[9] H. L. B. Boström, J. A. Hill, and A. L. Goodwin, "Columnar shifts as symmetry-breaking degrees of freedom in molecular perovskites," Phys. Chem. Chem. Phys. **18**, 31881–31894 (2016).
[10] H. L. B. Boström, "Tilts and shifts in molecular perovskites," CrystEngComm **22**, 961–968 (2020).
[11] H. L. B. Boström and A. L. Goodwin, "Hybrid Perovskites, Metal–Organic Frameworks, and Beyond: Unconventional Degrees of Freedom in Molecular Frameworks," Acc. Chem. Res. **54**, 1288–1297 (2021).
[12] H. L. B. Boström, M. S. Senn, and A. L. Goodwin, "Recipes for improper ferroelectricity in molecular perovskites," Nat. Commun. **9**, 2380 (2018).
[13] K. Hirakawa and Y. Kurogi, "One-Dimensional Antiferromagnetic Properties of $KCuF_3$," Prog. Theor. Phys. Supp. **46**, 147–161 (1970).
[14] S. K. Satija, J. D. Axe, G. Shirane, H. Yoshizawa, and K. Hirakawa, "Neutron scattering study of spin waves in one-dimensional antiferromagnet $KCuF_3$," Phys. Rev. B **21**, 2001–2007 (1980).
[15] D. A. Tennant, R. A. Cowley, S. E. Nagler, and A. M. Tsvelik, "Measurement of the spin-excitation continuum in one-dimensional $KCuF_3$ using neutron scattering," Phys. Rev. B **52**, 13368–13380 (1995).
[16] D. A. Tennant, S. E. Nagler, D. Welz, G. Shirane, and K. Yamada, "Effects of coupling between chains on the magnetic excitation spectrum of $KCuF_3$," Phys. Rev. B **52**, 13381–13389 (1995).
[17] H. J. Schulz, "Dynamics of Coupled Quantum Spin Chains," Phys. Rev. Lett. **77**, 2790–2793 (1996).
[18] B. Lake, D. A. Tennant, C. D. Frost, and S. E. Nagler, "Quantum criticality and universal scaling of a quantum antiferromagnet," Nat. Mater. **4**, 329–334 (2005).
[19] B. Lake, D. A. Tennant, J.-S. Caux, T. Barthel, U. Schollwöck, S. E. Nagler, and C. D. Frost, "Multispinon Continua at Zero and Finite Temperature in a Near-Ideal Heisenberg Chain," Phys. Rev. Lett. **111**, 137205 (2013).
[20] K.-L. Hu, M. Kurmoo, Z. Wang, and S. Gao, "Metal–Organic Perovskites: Synthesis, Structures, and Magnetic Properties of $[C(NH_2)_3][M^{II}(HCOO)_3]$ (M=Mn, Fe, Co, Ni, Cu, and Zn; $C(NH_2)_3$= Guanidinium)," Chem. Eur. J. **15**, 12050–12064 (2009).
[21] A. Stroppa, P. Jain, P. Barone, M. Marsman, J. M. Perez-Mato, A. K. Cheetham, H. W. Kroto, and S. Picozzi, "Electric Control of Magnetization

and Interplay between Orbital Ordering and Ferroelectricity in a Multiferroic Metal–Organic Framework," Angew. Chem. Int. Ed. **50**, 5847–5850 (2011).
[22] A. Stroppa, "Polar and Magneto-Electric Properties of Anti-Ferrodistortive Ordered Jahn-Teller Distortions in a multiferroic metal-organic framework," J. Phys. Conf. Ser. **428**, 012029 (2013).
[23] Y. Tian, A. Stroppa, Y. Chai, L. Yan, S. Wang, P. Barone, S. Picozzi, and Y. Sun, "Cross coupling between electric and magnetic orders in a multiferroic metal-organic framework," Sci. Rep. **4**, 6062 (2014).
[24] M. T. Hutchings, E. J. Samuelsen, G. Shirane, and K. Hirakawa, "Neutron-Diffraction Determination of the Antiferromagnetic Structure of $KCuF_3$," Phys. Rev. **188**, 919–923 (1969).
[25] N. Tsukuda and A. Okazaki, "Stacking Disorder in $KCuF_3$," J. Phys. Soc. Jpn. **33**, 1088–1099 (1972).
[26] S. J. Clark, M. D. Segall, C. J. Pickard, P. J. Hasnip, M. I. Probert, K. Refson, and M. C. Payne, "First principles methods using CASTEP," Z. Kristall. **220**, 567–570 (2005).
[27] M. C. Payne, M. P. Teter, D. C. Allan, T. Arias, and J. D. Joannopoulos, "Iterative minimization techniques for ab initio total-energy calculations - molecular-dynamics and conjugate gradients," Rev. Mod. Phys. **64**, 1045–1097 (1992).
[28] H. J. Monkhorst and J. D. Pack, "Special points for Brillouin-zone integrations," Phys. Rev. B **13**, 5188–5192 (1976).
[29] J. P. Perdew, A. Ruzsinszky, G. I. Csonka, O. A. Vydrov, G. E. Scuseria, L. A. Constantin, X. Zhou, and K. Burke, "Restoring the Density-Gradient Expansion for Exchange in Solids and Surfaces," Phys. Rev. Lett. **100**, 136406 (2008).
[30] A. Tkatchenko and M. Scheffler, "Accurate molecular van der waals interactions from ground-state electron density and free-atom reference data," Phys. Rev. Lett. **102**, 073005 (2009).
[31] E. McNellis, J. Meyer, and K. Reuter, "Azobenzene at coinage metal surfaces: Role of dispersive van der Waals interactions," Phys. Rev. B **80**, 205414 (2009).
[32] B. G. Pfrommer, M. Cote, S. G. Louie, and M. L. Cohen, "Relaxation of crystals with the quasi-Newton method," J. Comput. Phys. **131**, 233–240 (1997).
[33] R. H. Byrd, J. Nocedal, and R. B. Schnabel, "Representations of quasi-newton matrices and their use in limited memory methods," Math. Prog. **63**, 129–156 (1994).
[34] G. P. Francis and M. C. Payne, "Finite basis set corrections to total energy pseudopotential calculations," J. Phys.-Condes. Matter **2**, 4395–4404 (1990).
[35] C. Capillas, E. S. Tasci, G. de la Flor, D. Orobengoa, J. M. Perez-Mato, and M. I. Aroyo, "A new computer tool at the Bilbao crystallographic server to detect and characterize pseudosymmetry," Z. Kristall. **226**, 186–196 (2011).
[36] Z. Yang, G. Cai, C. L. Bull, M. G. Tucker, M. T. Dove, A. Friedrich, and A. E. Phillips, "Hydrogen-bond-mediated structural variation of metal guanidinium formate hybrid perovskites under pressure," Phil. Trans. R. Soc. A **377**, 20180227 (2019).
[37] B. J. Campbell, H. T. Stokes, D. E. Tanner, and D. M. Hatch, "ISODISPLACE: a web-based tool for exploring structural distortions," J. Appl. Crystallogr. **39**, 607–614 (2006).
[38] A. Stroppa, P. Barone, P. Jain, J. M. Perez-Mato, and S. Picozzi, "Hybrid Improper Ferroelectricity in a Multiferroic and Magnetoelectric Metal-Organic Framework," Adv. Mat. **25**, 2284–2290 (2013).
[39] I. E. Collings, J. A. Hill, A. B. Cairns, R. I. Cooper, A. L. Thompson, J. E. Parker, C. C. Tang, and A. L. Goodwin, "Compositional dependence of anomalous thermal expansion in perovskite-like ABX_3 formates," Dalton Trans. **45**, 4169–4178 (2016).
[40] N. L. Evans, P. M. M. Thygesen, H. L. B. Boström, E. M. Reynolds, I. E. Collings, A. E. Phillips, and A. L. Goodwin, "Control of Multipolar and Orbital Order in Perovskite-like $[C(NH_2)_3]Cu_xCd_{1-x}(HCOO)_3$ Metal–Organic Frameworks," J. Am. Chem. Soc. **138**, 9393–9396 (2016).
[41] B. Fultz, "Vibrational thermodynamics of materials," Prog. Mater Sci. **55**, 247–352 (2010).
[42] S. Burger, S. Grover, K. T. Butler, H. L. B. Boström, R. Grau-Crespo, and G. Kieslich, "Tilt and shift polymorphism in molecular perovskites," Mater. Horiz. **8**, 2444–2450 (2021).
[43] K. Li, Z.-G. Li, J. Xu, Y. Qin, W. Li, A. Stroppa, K. T. Butler, C. J. Howard, M. T. Dove, A. K. Cheetham, and X.-H. Bu, "Origin of Ferroelectricity in Two Prototypical Hybrid Organic–Inorganic Perovskites," J. Am. Chem. Soc. **144**, 816–823 (2022).